Electronic structure of layered $1T$-$TaSe_2$ in commensurate charge-density-wave phase studied by angle-resolved photoemission spectroscopy

Y. Aiura* and H. Bando
National Institute of Advanced Industrial Science and Technology, Tsukuba, Ibaraki 305-8568, Japan

R. Kitagawa, S. Maruyama, and Y. Nishihara
Faculty of Science, Ibaraki University, Mito, Ibaraki 310-8512, Japan

K. Horiba, M. Oshima, and O. Shiino†
Department of Applied Chemistry, University of Tokyo, Tokyo 113-8656, Japan

M. Nakatake
Institute of Materials Structure Science, Tsukuba, Ibaraki 305-0801, Japan
(Received 6 February 2003; published 29 August 2003)

We present a detailed angle-resolved photoemission study of the electronic structure of layered $1T$-$TaSe_2$ in the commensurate charge-density-wave (CDW) phase. A considerable reduction in the spectral weight of a quasiparticle band centered at the binding energy of about 0.25 eV below the Fermi level is observed in the momentum space ranging from the end of the first surface Brillouin zone to the second surface Brillouin zone. Moreover, no crossings of the Fermi level are visible in the whole Brillouin zone, meaning that the Fermi level lies in a pseudogap created by the tails of two overlapping Hubbard subbands. Our results indicate that not only the electron-phonon coupling, which is responsible for the formation of the CDW, but also the subsequent electron correlation effects in the Ta $5d$ band play an important role for the establishment of electronic structure of $1T$-$TaSe_2$ in the commensurate CDW phase.

DOI: 10.1103/PhysRevB.68.073408 PACS number(s): 71.20.−b, 71.45.Lr, 79.60.−i

The layered transition metal dichalcogenides $1T$-TaS_2 and $1T$-$TaSe_2$ have attracted much attention because of their quasi two dimensionality (2D) and, consequently, their unique physical properties leading to formation of the charge-density wave (CDW).[1] Although these two materials have the same CdI_2-type crystal structure and similar CDW superstructure, they show dramatically different physical properties. In particular, it was revealed in $1T$-TaS_2 that the metal-to-insulator transition from the quasicommensurate (metallic) CDW to the commensurate (insulating) CDW phase occurring at 180 K is closely related to a Mott localization induced by the electron correlation effects in the Ta $5d$ band.[2–4] Very recently, Pillo *et al.* studied the electronic structure of $1T$-TaS_2 in the quasicommensurate (metallic) CDW phase in detail using angle-resolved photoemission spectroscopy (ARPES).[5,6] They pointed out the importance of the electron correlation effects in the quasicommensurate (metallic) CDW phase. On the other hand, $1T$-$TaSe_2$ undergoes an incommensurate CDW to commensurate CDW transition at about 430 K without drastic change in the electronic conductivity in the whole commensurate CDW phase, and exhibits a metallic behavior.[2,7,8] Because of the larger interaction among the layers due to a large charge transfer between Ta $5d$ and Se $4p$ orbitals, $1T$-$TaSe_2$ has a three-dimensional (3D) character in the electronic structure[8–10] stronger than $1T$-TaS_2.[9–12] From this viewpoint, one may say that the Ta $5d$ electrons in $1T$-$TaSe_2$ may be less susceptible to localization.[13]

To elucidate these physical properties, it is essential to understand the role of the electron-phonon coupling, which is responsible for the occurrence of the CDW and the subsequent electron correlation effects in the Ta $5d$ band, in the electronic structure. Although the importance of the electron correlation effects in $1T$-TaS_2 has been recognized enough by virtue of various experimental techniques, such as scanning tunneling spectroscopy (STS)[14] and ARPES,[3–6,11] direct information about the occurrence of the CDW, that is, the crucial evidence for the nesting behavior on the 2D Fermi surface (FS) has yet to be reported. The influence of the electron correlation effect for $1T$-$TaSe_2$ in the CDW phase is expected to be smaller than that for $1T$-TaS_2 in the commensurate (metallic) CDW phase, because of the larger interaction between Ta $5d$ and Se $4p$ orbitals, as mentioned above. In other words, it is thought that the role of the electron-phonon coupling to the electron correlation effects for the electronic structure of $1T$-$TaSe_2$ becomes more important compared with that for $1T$-TaS_2. To investigate the interplay between the electron-phonon coupling and the electron correlation effects of the Ta $5d$ band on the electronic structure of $1T$-$TaSe_2$ in the commensurate CDW phase, we performed a detailed ARPES study.

ARPES measurements were carried out at BL-1C of the Photon Factory (KEK, Tsukuba) using an electron spectrometer mounted on a two-axis goniometer (VG ARUPS10).[15] The sample goniometer used here provides independent polar, azimuth, and tilt rotation of the sample.[16] All ARPES spectra were taken at the photon energy ($h\nu$) of 40 eV. The radiation was linearly polarized in the horizontal plane of incidence. The samples were mounted vertically and only photoelectrons emitted from the plane defined by the light beam and the surface normal were observed. The emission angle of the photoelectron measured from the surface normal

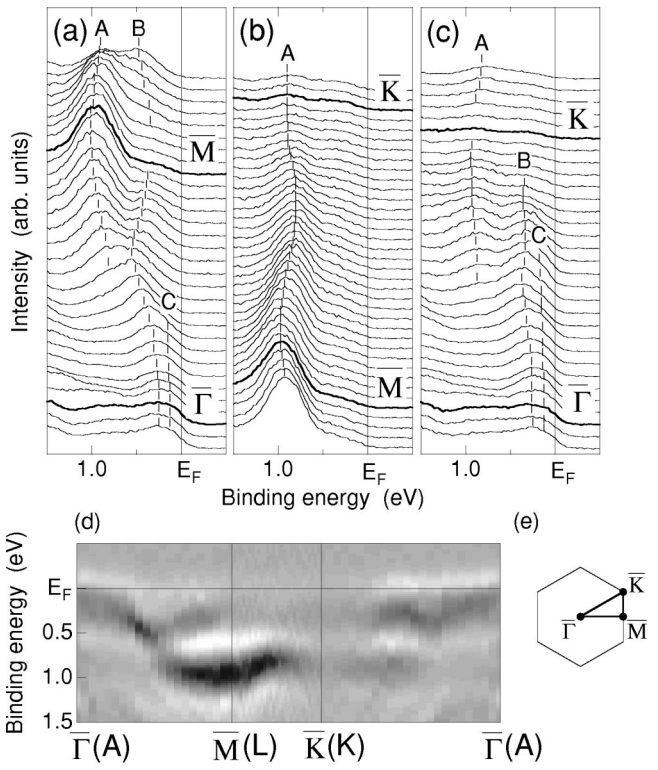

FIG. 1. EDC spectra of $1T$-$TaSe_2$ along the (a) $\overline{\Gamma M}$, (b) $\overline{MK}$, and (c) $\overline{\Gamma K}$ directions, taken with $h\nu=40$ eV at RT, and (d) the empirical band dispersion visualized by use of the second derivatives of the EDC spectra. The empirical bands are displayed in the linear gray scale plots, where the black regions denote the negative peak of the second derivatives. The notation in the parenthesis are the irreducible representations in the bulk BZ. (e) Drawing of the SBZ with the corresponding high-symmetry points for the CdI_2-type structure.

(θ_e) can be varied by rotating the sample along the polar axis or by rotating the energy analyzer horizontally. To avoid polarization effects of the light reported previously,[17] we rotated the energy analyzer and fixed the angle of incidence of the light (θ_I) to 45°. The azimuth angle (φ_e) was varied by rotating the samples to the surface normal. Single crystals of $1T$-$TaSe_2$ were grown by the iodine transport method.[7,8] The samples were cleaved *in situ* in an ultrahigh vacuum. The base pressure in the system was about 1×10^{-9} Torr. The angular resolution and the energy resolution were $\pm2°$ and about 150 meV, respectively.

Figure 1 shows energy distribution curves (EDC's) for $1T$-$TaSe_2$ along the high-symmetry directions (a) $\overline{\Gamma M}$, (b) $\overline{MK}$, and (c) $\overline{\Gamma K}$ of the surface Brillouin zone (SBZ) for the CdI_2-type structure and (d) the empirical band dispersion visualized by use of the second derivatives of the EDC spectra, respectively.[18] The empirical bands are displayed in linear gray scale plots, where the black regions denote the negative peak of the second derivatives. The EDC spectra at the Γ point denote normal emission and the $\overline{M}$ and $\overline{K}$ points in the SBZ correspond to parallel momenta of $k_\parallel=1.05$ and 1.21 Å^{-1}, respectively. At first sight, we find three distinct quasiparticle (QP) bands centered at the binding energy of about 0.9, 0.25, and 0.1 eV, denoted by A, B, and C, respectively in the EDC spectra. These QP bands can be explained by a gross distortion of the band structure due to the formation of the CDW superstructure.[19] Also, an exchange of the spectral weight between these QP bands along the $\overline{\Gamma M}$ direction is shown in Fig. 1(a). As a result of the exchange, it is shown in Fig. 1(d) that the center-of-gravity of the spectral weight disperses downward in energy along the $\overline{\Gamma M}$ direction. The empirical dispersive behavior along the $\overline{\Gamma M}$ direction is predicted by theoretical calculations in the normal state without the formation of the CDW,[9,10] which is very similar to that of $1T$-TaS_2 in the CDW phase.[5,11,19–21] This means that the overall shape of the electron wave functions along the $\overline{\Gamma M}$ direction is governed by the Fourier components of the crystal potential of the undistorted $1T$ lattice, rather than the CDW-related contribution.[21] In contrast, such an exchange behavior of the spectral weight is not seen along the $\overline{MK}$ direction, only band A appears around the $\overline{M}$ point, as shown in Figs. 1(b) and 1(d).

In order to get more detailed information about the actual behavior of these QP bands near the $\overline{MK}$ direction, we measured azimuth dispersion spectra through the first and the second SBZ for the different parallel momenta, as shown in Fig. 2. The data start near the $\overline{\Gamma M}$ direction and end near the next $\overline{\Gamma M}$ direction through the $\overline{\Gamma M'}$ direction.[22] Each azimuth scan has been carried out along one of the arcs shown in the bottom right sketch of Fig. 2. The parallel momentum on the top right of each dispersion spectra corresponds to the radius of the azimuth scan. In Fig. 2, the azimuth spectra show no significant polarization effects of the light along the $\overline{KMK}$ and $\overline{KM'K}$ lines[17] because θ_I was kept constant (45°) during the measurement. This facilitates the following discussion. In these azimuth dispersion spectra, one observes two bands A and B, but not band C, which is shown around the Γ point in Fig. 1. The bands A and B show significant modulation with parallel momentum. At $k_\parallel=0.64$ Å^{-1}, the band B dominates the spectral shape. The band A appears in the azimuth spectra at $k_\parallel=0.74$ Å^{-1}. As we go from $k_\parallel=0.74$ to 0.95 Å^{-1}, the spectral weight of the band A increases and that of the band B decreases gradually. Then, the band B becomes faint at $k_\parallel=1.05$ Å^{-1}. The considerable reduction in the spectral weight of the band B is shown in the momentum region from $k_\parallel=1.05$ to 1.24 Å^{-1}. Finally, the band B reappears in the azimuth spectra at $k_\parallel=1.34$ Å^{-1} and $k_\parallel=1.44$ Å^{-1}.

In order to corroborate the reduction in the spectral weight of the band B, we showed (parallel) momentum distributions of the spectral weight at the binding energy (E_B) of (a) 100, (b) 200, (c) 400, (d) 600, (e) 800, and (f) 1000 meV in Fig. 3. The topology of the Fermi surface, or the momentum distribution of the spectral weight at $E_B=0$ meV (not shown) is almost consistent with that at $E_B=100$ meV. White and black corresponds to high and low spectral weight, respectively. The momentum distributions of the spectral weight at $E_B=100$, 200, and 400 meV are induced by band B and those at $E_B=600$, 800, and 1000 meV are induced by band A. For the sake of convenience, the distributions of the high spectral weight at each binding en-

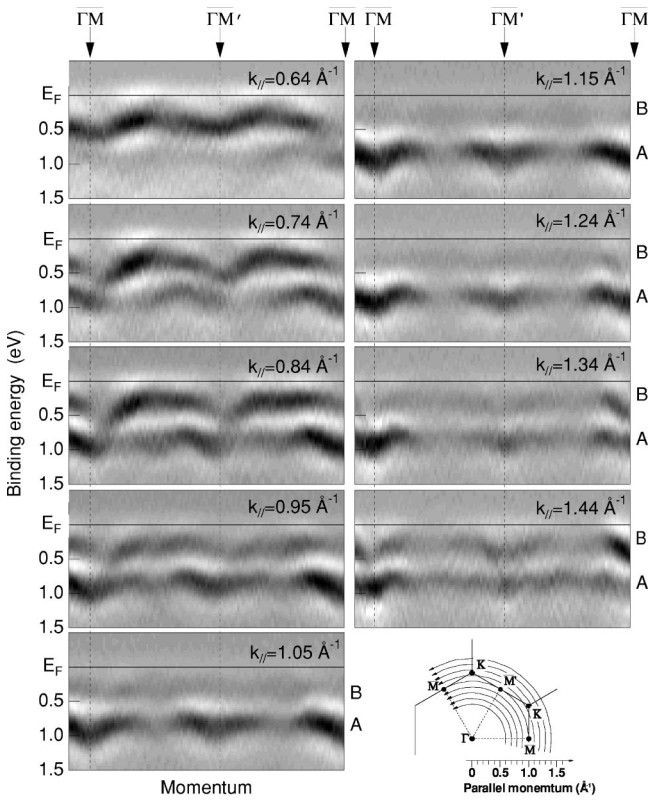

FIG. 2. Azimuth dispersion spectra of $1T$-$TaSe_2$ through the first SBZ and the second SBZ for the different parallel momenta, taken with $h\nu = 40$ eV at RT. Spectra visualized by use of the second derivatives start near the $\overline{\Gamma M}$ direction and end near the next $\overline{\Gamma M}$ direction through the $\overline{\Gamma M'}$ direction. Bottom right: Sketch of the arcs where spectra have been taken with the fixed parallel momenta indicated.

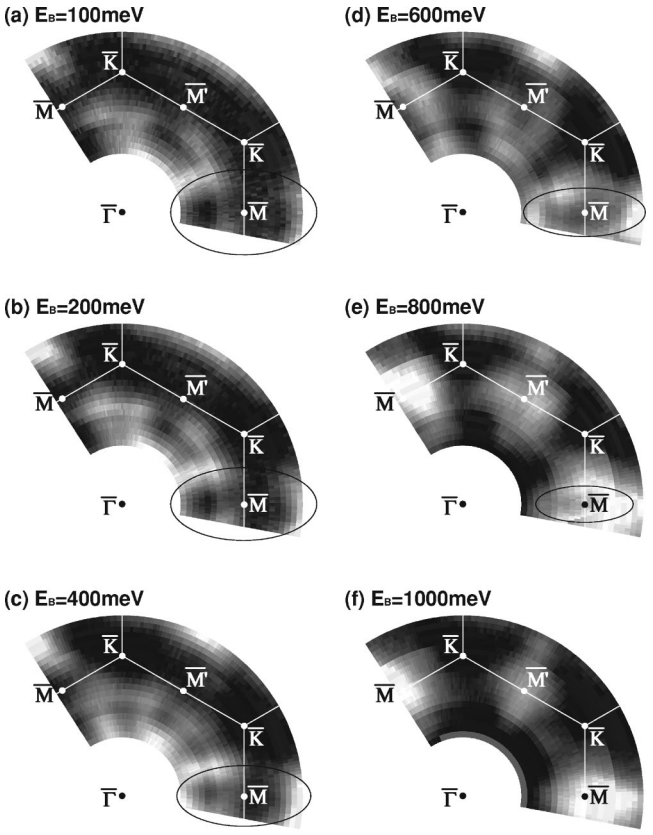

FIG. 3. Momentum distributions of the spectral weight of $1T$-$TaSe_2$ at the binding energy of (a) 100, (b) 200, (c) 400, (d) 600, (e) 800, and (f) 1000 meV. White and black corresponds to high and low spectral weight, respectively. The SBZ and the high-symmetry points are indicated.

ergy are shown by means of an arbitrary ellipse centered at the $\overline{M}$ point in Fig. 3. The extension of the ellipses from the bands A and B reduces gradually with increasing binding energy. This behavior is qualitatively consistent with the prediction of theoretical calculations in the normal state without the formation of the CDW, showing an electron pocket around the $\overline{M}$ point.[9,10,12] As shown in Figs. 3(a), 3(b), and 3(c), however, a considerable reduction in the spectral weight of the band B is shown in the momentum space for the area between the end of the first SBZ and the second SBZ. Very recently, Pillo *et al.* observed similar behavior with respect to the band B for $1T$-TaS_2 in the quasicommensurate CDW and commensurate CDW phases, showing that a considerable reduction in the spectral weight of the band B occurs around the $\overline{M}$ point.[5]

Based on a theoretical picture where the nesting of the Fermi surface plays a key role in the formation of the CDW, it is considered that the observed reduction in the spectral weight of band B is ascribed to the CDW-induced energy gap. From previous tunneling studies for $1T$-$TaSe_2$, it was reported that the values of CDW-induced energy gap $2\Delta_{CDW}$ are about 0.3 (Ref. 23) and 0.5 eV.[24] The size of these energy gaps is almost consistent with the binding energy of the band B (0.25 eV). However, there are two questions about this nesting scenario. First, the locations in the momentum space where the drastic reduction in the spectral weight of the band B occurs are different for $1T$-$TaSe_2$ and $1T$-TaS_2. This should be explained in terms of the difference in the dimensionality.[8–11] The electronic structure of $1T$-TaS_2 is independent of the momentum normal to the layers ($k_\perp$) due to negligibly small charge transfer between Ta $5d$ and S $3p$ orbitals,[11] resulting in the highly 2D character.[9,10] On the other hand, the electronic structure of $1T$-$TaSe_2$ depends on $k_\perp$ because of a large charge transfer between Ta $5d$ and Se $4p$ orbitals.[8–10] In order to confirm the $k_\perp$ effects on the nesting of the FS for $1T$-$TaSe_2$, further ARPES experiments are required using various photon energies. The other question is that the size of the energy gap is inconsistent with that predicted by mean-field (MF) theory. Using the binding energy of the band B for Δ_{CDW} (0.25 eV) and the transition temperature (T_{CDW}) of 600 K used in Ref. 23, $2\Delta_{CDW}/k_B T_{CDW}$ is estimated to be 9.7, indicating strong coupling in the CDW phase, where k_B is Boltzmann's constant.

The strong coupling behavior is supposed to be caused by the electron correlation effects in the Ta $5d$ band.[23] For 1-TaS_2 in the quasicommensurate (metallic) CDW phase, previous ARPES studies showed that no crossings of the Fermi level are visible in the complete Brillouin zone, result-

ing in a pseudogap of the FS.[5,6] It was concluded that the pseudogap behavior is induced by the electron correlation effects in the Ta $5d$ band. Our ARPES spectra for $1T$-$TaSe_2$ in the commensurate CDW phase also shows no crossings of the Fermi level, as shown in Figs. 1 and 2. For $h\nu = 40$ eV used here, the $\bar{\Gamma}\bar{M}$ line in the first SBZ almost corresponds to the AL line in the bulk BZ, assuming a work function of 4.5 eV and an inner potential of 12.2 eV.[8] Along the AL line, band calculations predict one-particle Ta $5d$ band crossing the Fermi level.[9,10] This means that the lack of bands crossing the Fermi level is not due to the 3D character of the electronic structure of $1T$-$TaSe_2$, but due to the electron correlation effects in the Ta $5d$ band, resulting in a pseudogap at the Fermi level created by the tails of two overlapping Hubbard subbands.

In our previous ARPES study, we concluded that $1T$-$TaSe_2$ has a 3D electronic structure from the normal emission spectra results along the ΓA direction.[8] From the previous results and the present ARPES results, one may say that the electronic structure of $1T$-$TaSe_2$ in the commensurate CDW phase can be described by the interplay of the electron correlation effects in the Ta $5d$ band and the large hybridization effects between Ta $5d$ and Se $4p$ orbitals which cause the observed 3D character.

We examined in detail the electronic band structure of $1T$-$TaSe_2$ in the commensurate CDW phase by means of ARPES. In particular, a considerable reduction in the spectral weight of the QP band centered at the binding energy of about 0.25 eV was shown in the momentum space ranging from the end of the first SBZ to the second SBZ. Moreover, no crossings of the Fermi level were shown in the complete Brillouin zone, which means that the Fermi level lies in a pseudogap created by the tails of two overlapping Hubbard subbands. Our results indicate that not only electron-phonon coupling, which is responsible for the formation of the CDW, but also the effects of subsequent electron correlation in the Ta $5d$ band play an important role for the establishment of electronic structure of $1T$-$TaSe_2$ in the commensurate CDW phase.

The authors have benefited from useful discussions with Dr. S. Koikegami. This work was partly done under Project No. 2002G174 at Institute of Material Structure Science in KEK.

*Electronic address: y.aiura@aist.go.jp
†Present address: Data Storage Technology Center, TDK corporation, Saku 385-0009, Japan.

[1] J.A. Wilson and A.D. Yoffe, Adv. Phys. **18**, 193 (1969).
[2] P. Fazekas and E. Tossatti, Philos. Mag. B **39**, 229 (1979); Physica B **99**, 183 (1980).
[3] R. Manzke *et al.*, Europhys. Lett. **8**, 195 (1985).
[4] B. Dardel *et al.*, Phys. Rev. B **45**, 1462 (1992); **46**, 7407 (1992).
[5] Th. Pillo *et al.*, Phys. Rev. B **62**, 4277 (2000); P. Aebi *et al.*, J. Electron Spectrosc. Relat. Phenom. **117-118**, 433 (2001).
[6] Th. Pillo *et al.*, Phys. Rev. Lett. **83**, 3494 (1999); Th. Pillo *et al.*, J. Electron Spectrosc. Relat. Phenom. **101-103**, 811 (1999).
[7] K. Horiba *et al.*, Surf. Rev. Lett. **9**, 1085 (2002).
[8] K. Horiba *et al.*, Phys. Rev. B **66**, 073106 (2002).
[9] H.W. Myron and A.J. Freeman, Phys. Rev. B **11**, 2735 (1975).
[10] A.M. Woolley and G. Wexler, J. Phys. C **10**, 2601 (1977).
[11] Th. Pillo *et al.*, Phys. Rev. B **64**, 245105 (2001).
[12] L.F. Mattheiss, Phys. Rev. B **8**, 3719 (1973).
[13] A recent ARPES work on $1T$-$TaSe_2$ reported that a metal-insulator Mott transition occurs at the surface, which is driven by the localization of the Ta $5d$ band at the surface; L. Perfetti *et al.*, Phys. Rev. Lett. **90**, 166401 (2003).
[14] J.-J. Kim *et al.*, Phys. Rev. Lett. **73**, 2103 (1994); J.-J. Kim *et al.*, Phys. Rev. B **56**, 15 573 (1997).
[15] K. Ono *et al.*, Nucl. Instrum. Methods Phys. Res. A **467**, 573 (2001); K. Ono *et al.*, *ibid.* **467**, 1497 (2001).
[16] The sample goniometer used here is constructed for motorized, computer-controlled data acquisition and can be cooled with LHe down to 12.5 K (R-Dec Co. Ltd., *i* GONIO LT); Y. Aiura *et al.*, Rev. Sci. Instrum. **74**, 3177 (2003).
[17] T. Greber *et al.*, Phys. Rev. B **45**, 4540 (1992); P. Aebi *et al.*, Surf. Sci. **307-309**, 917 (1994); Th. Pillo *et al.*, J. Electron Spectrosc. Relat. Phenom. **97**, 243 (1998).
[18] The second derivative method has been widely used and outlined the band dispersions excellently from EDC spectra. For example, see H. Kumigashira *et al.*, Phys. Rev. B **56**, 13 654 (1997); A. Ino *et al.*, *ibid.* **65**, 094504 (2002).
[19] N.V. Smith *et al.*, J. Phys. C **18**, 3175 (1985).
[20] R. Manzke *et al.*, J. Phys. C **21**, 2399 (1988).
[21] R. Claessen *et al.*, Phys. Rev. B **41**, 8270 (1990).
[22] Because of the space group D_{3d}^3 for the CdI_2-type structure, we have to distinguish between the $\bar{M}$ point and $\overline{M'}$ in the SBZ, where the $[\overline{\Gamma M'}]$ direction is defined by the direction for which the chalcogenide atom is located in the surface layer; N.V. Smith and M.M. Traum, Phys. Rev. B **11**, 2087 (1975); M.M. Traum *et al.*, Phys. Rev. Lett. **32**, 1241 (1974).
[23] C. Wang *et al.*, Phys. Rev. B **42**, 8890 (1990).
[24] S. Noutomi *et al.*, Solid State Commun. **50**, 181 (1984).